LETTER • OPEN ACCESS

Multidecadal variability of ENSO in a recharge oscillator framework

View the article online for updates and enhancements.

ENVIRONMENTAL RESEARCH
LETTERS

LETTER

CrossMark

Multidecadal variability of ENSO in a recharge oscillator framework

Lander R Crespo[1] , Mª Belén Rodríguez-Fonseca[2,3,*] , Irene Polo[2] , Noel Keenlyside[1] and Dietmar Dommenget[4,5]

[1] Geophysical Institute, University of Bergen and Bjerknes Centre for Climate Research, Postboks 7803, 5020 Bergen, Norway
[2] Department of Earth Physics and Astrophysics, UCM, Plaza de las Ciencias, 28040 Madrid, Spain
[3] Instituto de Geociencias (IGEO), CSIC-UCM, Madrid, Spain
[4] ARC Centre of Excellence for Climate Extremes, Australia
[5] School of Earth, Atmosphere and Environment, Monash University, Clayton, VIC 3800, Australia
[*] Author to whom any correspondence should be addressed.

E-mail: brfonsec@ucm.es

Abstract

We use a conceptual recharge oscillator model to identify changes in El Niño and the Southern Oscillation (ENSO) statistics and dynamics during the observational record. The variability of ENSO has increased during the 20th century. The cross-correlation between sea surface temperature (SST) and warm water volume (WWV) has also changed during the observational record. From the 1970s onwards, the SST drives WWV anomalies with a lead-time of ten months and the WWV feedbacks onto the SST with a lead-time of eight months. This is reminiscent of a recharge-discharge mechanism of the upper ocean heat content. The full recharge-discharge mechanism is only observed from the 1970s onwards. This could be the result of the degradation of the quality of observations in the early part of the 20th century. However, it may also be a consequence of decadal changes in the coupling between WWV and SST. Additional analysis fitting the recharge oscillator model to the coupled state-of-the-art climate models indicates that ENSO properties show little decadal changes in the climate models. The disagreement in changes in ENSO properties between the reanalysis and the climate models can be due to errors in the available observational data or due to the models missing the low frequency variability and decadal wind trends. Longer and more reliable observational records would be required to validate our results.

1. Introduction

El Niño and the Southern Oscillation (ENSO) is the dominant mode of interannual climate variability and it has major global impacts. ENSO phenomenon can be well characterized by the following set of properties: frequency, amplitude, spatial structure of the sea surface temperature (SST) anomalies and length of the event. The characteristics of ENSO change on decadal to interdecadal timescales and they can be modulated by Pacific internal variability (Kirtman and Schopf 1998, An and Wang 2000, Fedorov and Philander 2001, Wang and An 2001, Philander and Fedorov 2003, Yeh and Kirtman 2004, Fedorov et al 2020), or by remote impacts from other basins (Yu et al 2002, Wu and Kirtman 2004, Yeh and Kirtman 2004, Annamalai et al 2005, Behera et al 2006, Dommenget et al 2006, Dong et al 2006, Yeh et al 2007, Polo et al 2008,

Jansen et al 2009, Rodriguez-Fonseca et al 2009, Ding et al 2012, Frauen and Dommenget 2012, Ham et al 2013, Martín-Rey et al 2014, 2015, Polo et al 2015, Dommenget and Yu 2017, Wang et al 2017, 2019, Cai et al 2019, Wang et al 2020). However, understanding such changes requires long observational records (Wittenberg 2009).

It is essential to understand the changes in ENSO properties such as frequency and intensity and the underlying dynamics causing them. The state-of-the-art climate models have been extensively used to explore ENSO dynamics and the relative contribution of the diverse feedbacks in play (Kug et al 2012, Bellenger et al 2014, Vijayeta and Dommenget 2018, Feng et al 2020). However, the Coupled Model Intercomparison Project (CMIP) models still show large biases with respect to observations and struggle to capture the right dynamics behind ENSO behavior. Most CMIP models represent ENSO as an SST-mode

(Guilyardi 2006), in contrast with the hybrid SST-and thermocline-mode present in the observations (Fedorov and Philander 2001). Feng *et al* (2020) find that a better simulation of the SST gradient over the western-central equatorial Pacific might allow a more reliable simulation of El Niño diversity in CMIP5 models.

Conceptual models are a powerful tool that can be used to condense the dynamics of ENSO in a simplified paradigm (Suarez and Schopf 1988, Jin 1997a, 1997b, Burgers *et al* 2005) and can help to understand the mechanisms behind the observed changes. The recharge oscillator model has been found to represent in a convenient way the Bjerknes Feedback and the dynamical coupling between SST and equatorial heat content (Jin 1997a, 1997b, Burgers *et al* 2005, Vijayeta and Dommenget 2018). The recharge oscillator theory was proven to be very useful to evaluate the representation of the feedback between SST and equatorial heat content in the CMIP models (Vijayeta and Dommenget 2018, Dommenget and Vijayeta 2019). The coefficients of the recharge oscillator model represent this mechanism and other properties such as variance of the key oceanic fields and frequency of ENSO events. The changes in the parameters over time can be related to changes in the background state of the atmosphere and ocean and be used for a better understanding of ENSO dynamics.

This study investigates the decadal changes in ENSO dynamics and statistics both in observations and climate model simulations during the 20th century. We use the recharge oscillator model (Jin 1997a, 1997b) in a simplified formulation (Burgers *et al* 2005) to provide robust statistics and insights on how changes in the background state alter the feedback components.

2. Data, model and experimental design

We use SST observations from Hadley Centre Global Sea Ice and Sea Surface Temperature version 1.1 (HadISST 1.1) dataset (Rayner *et al* 2003) with monthly temporal and $1° \times 1°$ spatial resolutions for the period 1900–2010. Thermocline depth is defined as the depth of the 20 °C isotherm (z20, hereafter) and is derived from 3D temperature field, taken from the ocean reanalysis SODA (Carton *et al* 2005) version 2.2.4 (Giese and Ray 2011) with monthly and $0.5° \times 0.5°$ resolutions from 1900 to 2010. We also use SST and z20 data from 35 CMIP5 models (Taylor *et al* 2012) for testing the recharge-discharge mechanism in a suite of higher complexity models. The Ocean Reanalysis of the 20th Century (ORA-20C) dataset is used to compare to our observational dataset. Nevertheless this dataset has limitations as it is designed to provide initial conditions for the ocean component of the CMWF 10-member ensemble of coupled climate reanalyses of the 20th century, from 1901-201

(CERA-20C) and not to explicitly explore climate signals (de Boisséson and Balmaseda 2016).

We use the simplified recharge oscillator model derived by Burgers *et al* (2005) (ReOsc model hereafter). The ReOsc model consists of two tendency equations for the two natural variables of the system, the SST anomalies averaged along the Niño3 (5° S–5° N, 150°–90° W) region, T_P, and the thermocline depth anomalies longitudinally averaged over the whole equatorial Pacific (5° S–5° N, 130° E–80° W), h_P. The thermocline depth is representative of the upper ocean warm water volume (WWV, hereafter). The monthly anomalies are computed with respect to the background state or climatological mean state, defined as the multi-year monthly mean

$$\frac{\mathrm{d}T_P}{\mathrm{d}t} = a_{11}T_P + a_{12}h_P + \xi_1$$
$$\frac{\mathrm{d}h_P}{\mathrm{d}t} = a_{21}T_P + a_{22}h_P + \xi_2. \tag{1}$$

The parameters in equation (1) are calculated with a multiple linear regression based on the ordinary least squares method (Burgers *et al* 2005, Jansen *et al* 2009, Frauen and Dommenget 2012). The regression coefficients a_{11} and a_{22} represent the damping/growing rate of T_P and h_P, respectively, while a_{12} and a_{21} account for the coupling between T_P and h_P. Stochastic white noises ξ_1 and ξ_2 force each model equation. The standard deviation of the stochastic noise forcing is estimated from the residual of the linear regression fit. Following Vijayeta and Dommenget (2018), we integrate the ReOsc model for 1000 year simulations with a timestep of 24 h, and we impose a decorrelation time of three days to the noises to mimic weather fluctuations that effectively result in white noise for monthly mean data. The results shown in this study are based on the statistics computed from the 1000 year ReOsc model runs.

3. Results

3.1. Observed changes in ENSO properties
ENSO properties show significant changes during the observational record (table 1). The variability of both WWV and SST is largest at the end of the 20th century compared to earlier periods. In contrast to the 1970–2000 period, the standard deviation of SST (WWV) is reduced by around 20% (38%) for the period 1935–1965, and by 11% (45%) for the period 1901–1931. These changes are beyond the 1%–2% (6%–9%) confidence intervals for SST (WWV) standard deviation.

The regression coefficients show significant changes between periods with a stronger coupling between T_P and h_P at the end of the 20th century. Also, the uncertainty in the coefficients is lower in the more recent period. The running-window cross-correlation between SST and WWV indicates

Table 1. Standard deviations of the HadISST-SODA dataset and of the ReOsc model (row 1–2) and regression coefficients of the ReOsc model (row 3–6) for the three study periods. The confidence limits for the standard deviations and uncertainties of the parameters are estimated from a bootstrap statistical procedure at a 95% significance level. Note that coefficient a_{12} is presented with one extra decimal digit to show that the coefficient changes between periods.

	ReOsc			HadISST-SODA2.2.4		
	1901–1931	1935–1965	1970–2000	1901–1931	1935–1965	1970–2000
std $T_{p\,(°C)}$	0.87 ± 0.01	0.78 ± 0.01	0.98 ± 0.01	0.72 ± 0.05	0.68 ± 0.05	0.97 ± 0.09
std $h_{p\,(m)}$	4.02 ± 0.06	4.55 ± 0.07	7.29 ± 0.09	4.39 ± 0.34	5.6 ± 0.34	7.66 ± 0.57
a_{11} (1/month)	-0.10 ± 0.05	-0.11 ± 0.05	-0.07 ± 0.03	N/A	N/A	N/A
a_{12} ($°C\,m^{-1}$/month)	0.011 ± 0.008	0.005 ± 0.007	0.017 ± 0.004	N/A	N/A	N/A
a_{21} ($m\,°C^{-1}$/month)	-0.64 ± 0.26	-0.71 ± 0.29	-1.01 ± 0.20	N/A	N/A	N/A
a_{22} (1/month)	-0.14 ± 0.05	-0.10 ± 0.04	-0.03 ± 0.03	N/A	N/A	N/A

that SST impacts WWV (i.e. negative lags) throughout the 20th century, with a maximum correlation of -0.5 to -0.65 at a lag of around six months before the 1960s and eight to ten months after the 1960s (figure 1). Thus, the impact of SST on surface winds and the essentially linear response of WWV to the winds have not changed substantially (figures 1(c)–(e), negative lags). In contrast, from 1901 to the 1960s the impact of WWV on SST (i.e. positive lags) is weak and the maximum lag month is hard to identify; thus WWV is not a good predictor for ENSO events during this period (figures 1(c) and (d)). Only after the 1970s there is a strong correlation when WWV leads SST by between five to ten months; the dynamics in this period resemble a recharge-oscillator with a first order asymmetric cross-correlation (figure 1(e)).

The periodicity of ENSO has also experienced changes along the 20th century. ENSO has gradually shifted towards shorter periods from a period of seven years (in 1901–1931 and 1935–1965) to a ~5 year period (in 1970–2000, figure 2(a)). The amplitude of the spectral peak is remarkably larger for the most recent period, indicating that ENSO has increased in energy in the latest decades analyzed (figures 2(a) and S1 (available online at stacks.iop.org/ERL/17/074008/mmedia)).

3.2. ENSO properties in the ReOsc model
The ReOsc reproduces the observed standard deviation in SST and WWV for the period 1970–2000, especially for SST (table 1). Both are not statistically distinguishable at the 5% level from the observations, according to a two-sided bootstrap test with 1000 model realizations. For the earlier periods, the model and the observations do not agree so well. The period 1901–1931 shows a quite good agreement in the standard deviation of the observed and simulated WWV but not in the SST, while the period 1935–1965 shows larger differences. During these earlier periods the model is not such a good fit to the data, as the simulated variability in both variables is statistically different to the observations at the 5% level. Nevertheless, the model simulates changes in the standard deviations of SST and WWV similar to the

observations. Thus, the recharge-oscillator dynamics may explain part of the multi-decadal changes in the ENSO variance.

The model broadly captures the observed changes in the lead-lag correlation of SST and WWV for the different periods (figure 1(b)). For the period 1901–1931, negative SST leads positive WWV by about six to eight months with a weaker simulated correlation than in the observations; while WWV and SST are hardly related when WWV leads in either model or observations (figure 1(c)). We find similar results for the period 1935–1965 with a good agreement between model and observations when SST leads WWV by five to six months with peak correlation of ~0.45. Again, the model is unable to capture the weak observed correlation values (~0.2) when WWV leads SST (figure 1(d)). The structure of both the observed and ReOsc cross-correlations for these two periods implies that SST variations (generated by noise in ReOsc) regulate equatorial heat content through ocean-atmosphere interaction, but that the heat content variations themselves do not substantially influence SST. This result implies a reduction of the dynamical coupling between the ocean and the atmosphere.

For the period 1970–2000, both observations and the ReOsc model show a strong recharge oscillator cycle. The model captures the timing of positive and negative cross-correlation peaks, though it has a weaker (stronger) correlation when SST leads (lags) WWV (figure 1(e)). Thus, during this period upper-ocean heat content can drive SST variations, which in turn can reverse the initial upper-ocean heat content anomalies through ocean–atmosphere interaction. Figure 1 shows how the representation of the full recharge-discharge mechanism improves considerably after the 1970s. These results are also reproduced using ORA-20C reanalysis. For positive lags, neither SODA nor ORA-20C (grey line in figure 1) present significant correlations in the first two periods in contrast to the high correlations from 1970 onwards (figures 1(c)–(e)). Note that SODA and ORA-20C use a different assimilation method, and their atmospheric forcings, ocean models and parameterizations are also different, which reinforces our result.
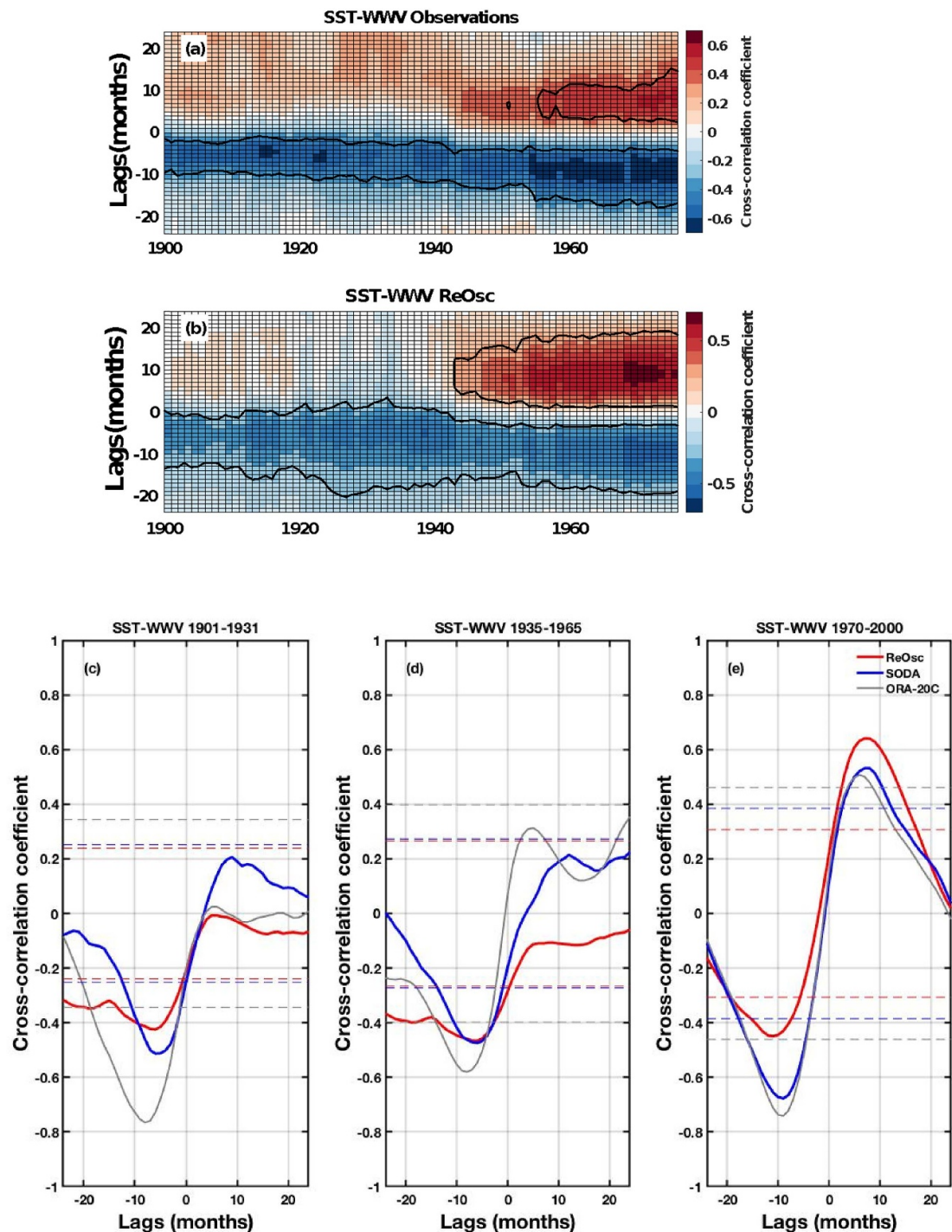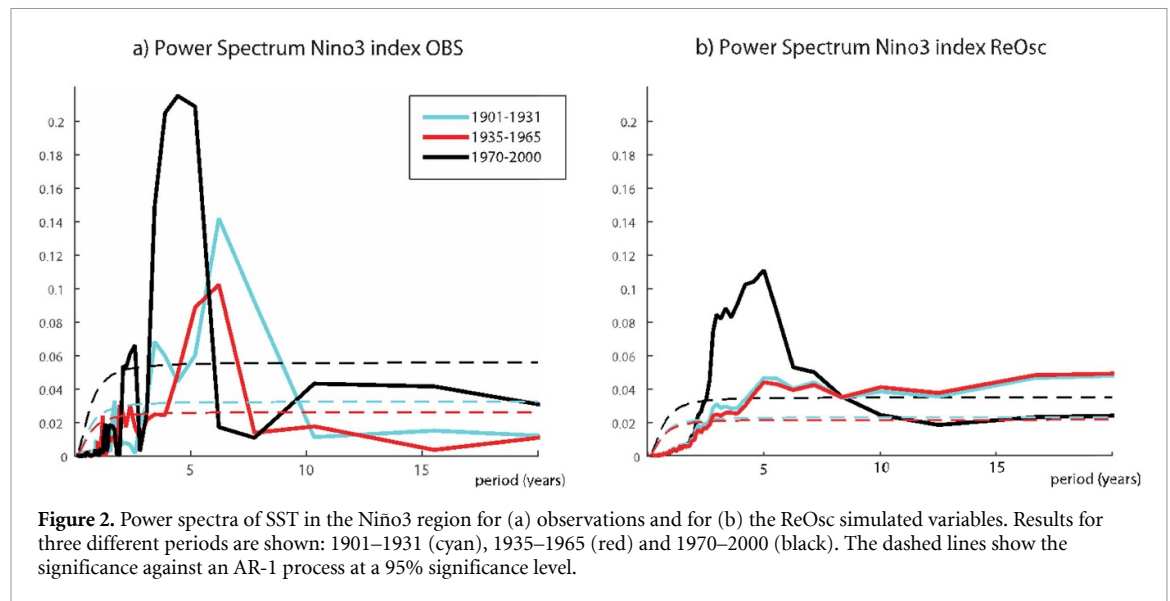
Figure 1. (a) Lead-lag cross-correlation of the simulated SST and WWV indices for 30 year running windows (we only show the first year in the *x*-axis) over the period 1901–2010 for (a) SODA reanalysis and (b) the ReOsc model. Positive (negative) lags in *y*-axis indicate that WWV leads (lags) SST. Negative and positive correlations are shown in blue and red shading. The significant values at a 95% significance level are contained within a solid black line contour. (c) Lead-lag cross-correlation of the reanalysis (blue line) and simulated (red line) SST and WWV indices for the period 1901–1931. (d) Same as c) but for 1935–1965. (e) Same as (c) for 1970–2000. The horizontal blue and red dashed lines indicate the confidence limits for observations and simulated variables, respectively, at a 95% significance level (computed following Sciremammano [1979]). Positive (negative) lags in *x*-axis indicate that WWV leads (lags) SST. The lead-lag cross-correlation between SST and WWV for ORA-20C reanalysis product (grey line, using ensemble mean of five members of ORA-20C) is also included together with the significance (horizontal grey dashed lines).

The changes in the model parameters may provide insight into the observed changes in ENSO properties, as the model largely reproduces the observed changes in SST and WWV variability and co-variability (table 1). The model parameters show

a substantial dependency on the period of analysis indicating that ENSO dynamics have considerably changed during the 20th century (table 1). The first two periods of analysis (1901–1931 and 1935–1965) present similar model parameter

Figure 2. Power spectra of SST in the Niño3 region for (a) observations and for (b) the ReOsc simulated variables. Results for three different periods are shown: 1901–1931 (cyan), 1935–1965 (red) and 1970–2000 (black). The dashed lines show the significance against an AR-1 process at a 95% significance level.

values (in agreement with the cross-correlation in figures 1(c) and (d)), but remarkable differences with respect to the latest period (1970–2000). The positive feedback of WWV onto SST anomalies, a_{12}, strengthens by 50% (240%) from the first (second) period to the latest period, indicating that upper-ocean heat content anomalies influence SST more strongly in the most recent period. The negative WWV coupling onto SST, a_{21}, also increases in 60% (40%), for the latest period in respect to the first (second) period (table 1). This result indicates that ocean–atmosphere interaction through the Bjerknes feedback (Bjerknes 1969) leads to stronger delayed heat content response. At the same time, the thermal damping of SST, a_{11}, reduces by 40% from the first and second periods to the most recent period; while the WWV damping, a_{22}, reduces by 70%–80%. The stronger coupling of WWV to SST in the period 1970–2000 and the weaker thermal damping can explain the good representation of the recharge mechanism (represented by the peak of WWV leading SST by ten months in figure 1(e)) and why the recharge oscillator model better describes the tropical Pacific upper ocean variability during this period. For the earlier periods the coupling between WWV and SST is weaker and thermal damping is stronger and thus the ENSO variability weakens and cannot be described well by the recharge oscillator model.
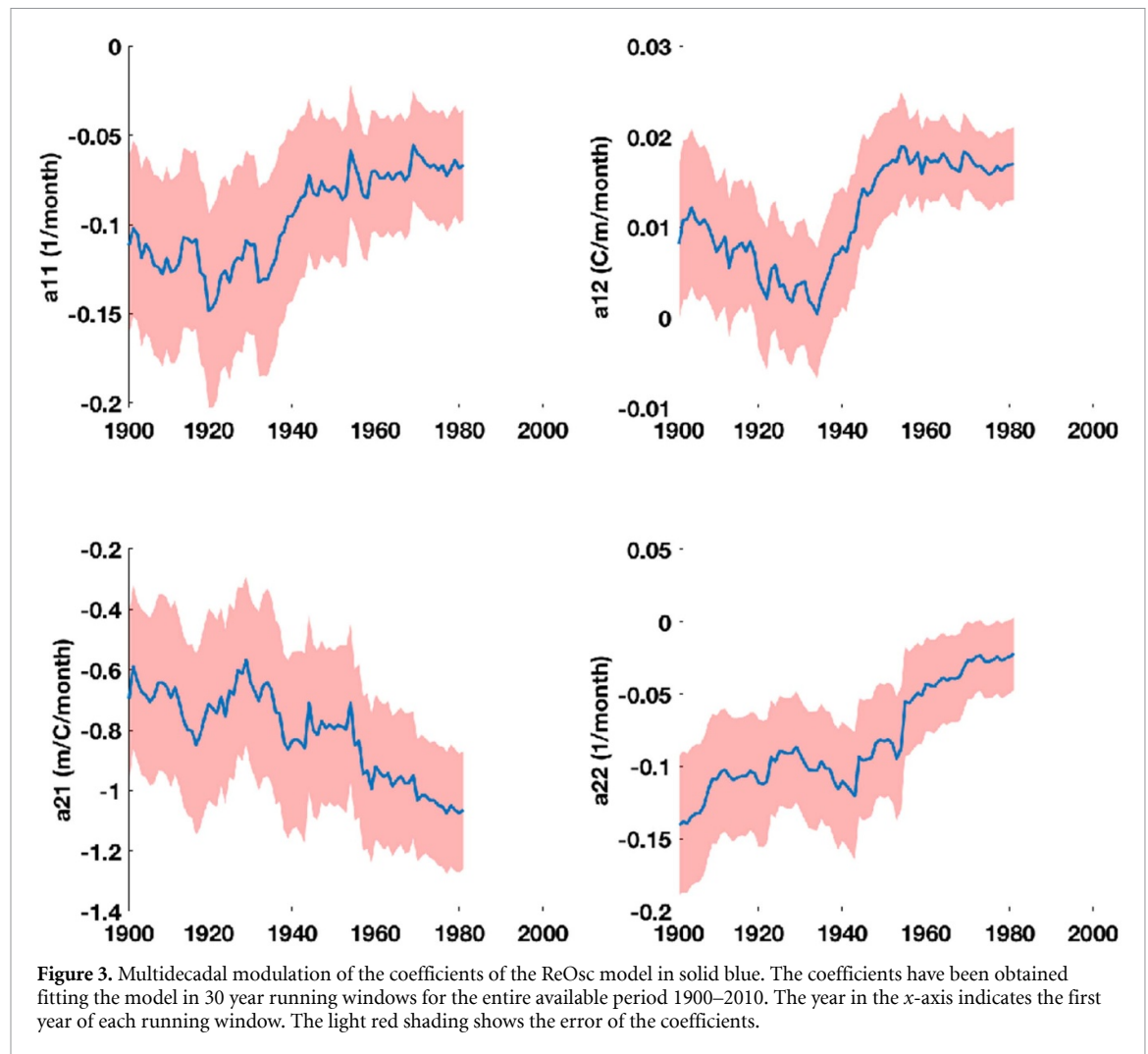
In the ReOsc simulations the main peak of periodicity is centered at five years and ranges from two to seven years, as in the observations for the period 1970–2000 (figure 2(b)). However, the ReOsc model fails to capture the periodic behavior of ENSO during the early periods (1900–1965). The ReOsc model simulates red-noise spectra during 1900–1931 and 1935–1965 without peaks around five to seven years.

The changes in the ReOsc model along the study period must be related with changes in the parameters of the model. We run the model sequentially from 1900 to 2010 carrying out the fitting to observations in 30 year running windows to obtain a continuous set of parameters representative of all epochs of the 20th century. In this way we are able to identify how the parameters representative of the dynamics of the model change and how these changes are related to the observed changes of ENSO properties. The evolution in time of these parameters could be used as decadal time series that shed light about possible modulators. The SST and WWV damping coefficients, a_{11} and a_{22} respectively, decrease monotonically hinting at a less damped ENSO system in recent decades (figures 3(a) and (d)), as can be seen in their evolution towards zero values. The coupling coefficients between SST and WWV (a_{12} and a_{21}) show an increasing trend (figures 3(b) and (c)) in recent decades (figures 3(b) and (c)). In particular the impact of the WWV on the SST (coefficient a_{12}) presents the largest multidecadal changes during the observational record and is likely the main driver of the observed changes of ENSO properties.

3.3. ENSO properties in the CMIP5 models
We use the ReOsc model fitted to the output of 35 different CMIP5 models to investigate whether the different types of dynamics during different periods seen in observations and reanalysis products can be found in climate model simulations. In addition, CMIP5 models present different background conditions that could help us to shed light about the decadal observed changes in ENSO properties.

Figure 4 shows eight models representative of the different dynamics found in the models (figure S2 shows the 35 models). There is a large

Figure 3. Multidecadal modulation of the coefficients of the ReOsc model in solid blue. The coefficients have been obtained fitting the model in 30 year running windows for the entire available period 1900–2010. The year in the *x*-axis indicates the first year of each running window. The light red shading shows the error of the coefficients.
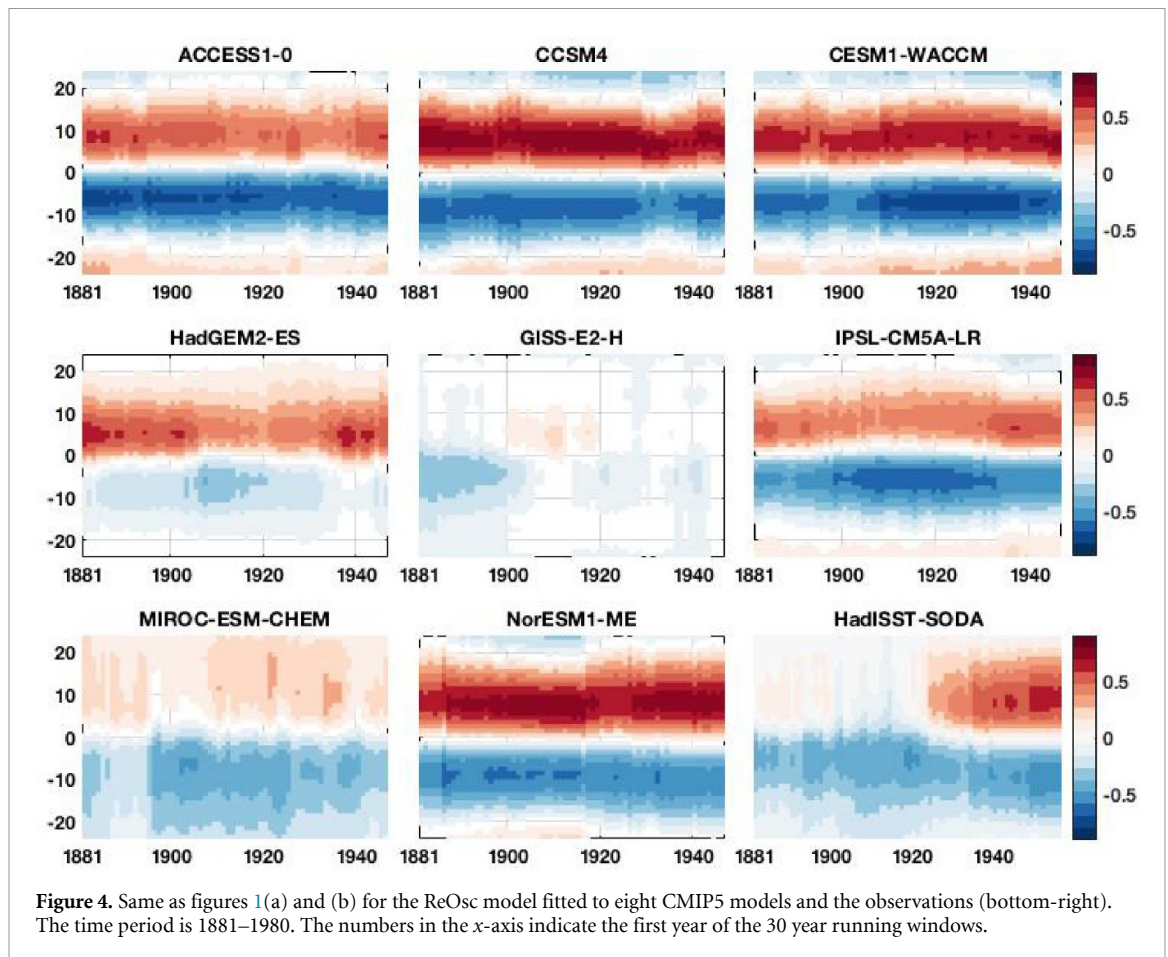
inter-model spread in the relationship between SST and WWV. Most CMIP5 models capture the full recharge-discharge mechanism, although a few completely miss the impact of WWV onto the SST (GISS-E2-H) or show a rather weak correlation (MIROC-ESM-CHEM). The representation of ENSO in those models is independent of subsurface ocean dynamics and they might be thermodynamically driven (Clement *et al* 2011). Some models have a stationary relationship along the whole period (CCSM4 and NorESM1-ME) while other models do show multidecadal variability in SST-WWV coupling (ACCESS1-0, CESM1-WACCM, HadGEM2-ES and IPSL-CM5A-LR) as we find in the observations. However, the multidecadal changes in the variance are overall smaller than in observations (figure S3).

We can classify the models into two different categories according to the strength of the SST-WWV two-way feedback. MIROC-ESM-CHEM and GISS-E2-H present a weak coupling while CESM1-WACCM and CCSM4 are a good example of strongly coupled models. The strength of the coupling is related to the magnitude of the SST variance in the equatorial Pacific; the stronger the coupling the

larger the variance, especially in the eastern equatorial Pacific (not shown). Similarly, strongly coupled models present larger peaks of periodicity representative of a larger spectral amplitude, in stark contrast to the models with weak coupling having low power spectra (not shown).

The coefficients of the ReOsc model also present multidecadal changes in the CMIP5 models but there is no inter-model agreement on the amplitude and sign of the change. The models do not show consistent changes as there is a lot of spread among the models in the parameters a_{11}, a_{12}, and a_{22} (figure S4), in contrast to the observations in which the feedback of WWV on SST is the main source of multidecadal variability as shown by the recharge-oscillator model.

This disagreement with reanalysis could be linked to model underrepresentation of low frequency variability and decadal wind trends in the Pacific Ocean (Kajtar *et al* 2018, McGregor *et al* 2018). Nevertheless, some models do show some multidecadal changes and, in addition, models with stronger coupling between h_{p} and T_{p} present stronger variability in the equatorial Pacific (not shown), in agreement with the changes in variance shown in table 1.

Figure 4. Same as figures 1(a) and (b) for the ReOsc model fitted to eight CMIP5 models and the observations (bottom-right). The time period is 1881–1980. The numbers in the *x*-axis indicate the first year of the 30 year running windows.

4. Discussion

We identify and quantify the multidecadal variability of ENSO dynamics and properties during the 20th century. We show that ENSO can be divided into two distinct regimes. From 1901 to 1965, the coupling between ocean and atmosphere is weaker and thus the variability of ENSO is reduced. From 1970 to 2010 the dynamic coupling between ocean and atmosphere at the equatorial Pacific is stronger and the variability is enhanced. ENSO dynamics can be accurately explained by a recharge-discharge mechanism of the Pacific upper ocean heat content for this period, but not for the earlier periods. This could suggest that WWV is only a good predictor for ENSO events since the 1970s. However, recent studies have found that in the period between 2000 and 2019 the impact of WWV onto the SST has weakened respect to previous decades (Hu *et al* 2020, Li *et al* 2020). There is no data available to explore if this is also the case in our dataset which extends only until 2010, so we are not able to confirm the possible changes occurring after 2000.

The changes in the ReOsc parameters also indicate that ENSO dynamics have changed throughout the 20th century. Those parameters indicate that, for the most recent period, the thermal damping is weaker, the influence of the upper-ocean heat

content anomalies in the SST stronger and that the delayed heat content response on SST is also stronger. For the earlier periods (1901–1965) the weaker coupling between WWV and SST and the stronger thermal damping weaken the ENSO variability. ENSO dynamics have clearly changed since the climate shift in the 1970s favoring a stronger thermocline feedback and a weaker zonal advective feedback (An and Jin 2000, An and Wang 2000, An 2009, Timmermann *et al* 2018), which is consistent with the observed increase in periodicity and variability. The simplified ReOsc model used here represents a coupled mode, based on the thermocline feedback, and does not include the zonal advective feedback (Fang and Zheng 2018). Thus, it is consistent that the ReOsc fits the observations better from 1970s onwards. It is hard to interpret the actual mechanism behind the changes in observations, but it is likely related to changes in the background state causing fluctuations in the parameter a_{12}, representative of the impact of WWV onto SST.

ENSO has gradually become more frequent changing from a seven-year periodicity in the beginning of 20th century to a five-year periodicity in the most recent decades included in our study. The energy of ENSO events has also increased in the recent decades with respect to early and mid 20th century periods. The ReOsc does not capture the changes in

periodicity but it reproduces the increase in the spectral energy. However, An and Wang (2000) found that in the late 1970s ENSO periodicity increased from 3–4 years to 4–6 years. In a wavelet analysis (see figure S1) we find the same shift in ENSO periodicity in the observations, but the presence of a strong peak of three-year periodicity in the late 90s results in an overall increased in periodicity for the period 1970–2000 (as shown in figure 2).

Note that the data for our model for the first half of the 20th century is entirely based on reanalysis since there are no available observations of subsurface ocean temperature prior to 1950. The feedback between SST and WWV also presents multidecadal variability in the ORA-20C reanalysis dataset and it is very similar to the HadISST-SODA dataset for the period 1970–2000. However, the amplitude of the cross-correlations are different for the periods 1901–1931 and 1935–1965, suggesting that there is a large uncertainty and differences across datasets for the earlier periods (figure 1). Bear in mind that ORA-20C shows a large spread in the first part of the century and it is strongly constrained by means of data assimilation towards an ocean state that is comparable with other reanalysis products. Dealing with the transition between the poorly observed early 20th century and the well-sampled later decades is a major challenge to take up before a product such as ORA-20C can be used for the detection of robust climate signals in the ocean subsurface (de Boisséson and Balmaseda 2016). A reconstruction of WWV back to 1950 based on sea level data supports our findings as they indicate that WWV is a poor predictor for SST prior to 1973 (Bunge and Clarke 2014). Also, we find similar changes in ENSO feedbacks between SST and WWV when we force the ReOsc model with a dataset built from a coupled ocean-atmosphere simulation with NorESM with observed wind stress prescribed globally (see figure S5). This is an indicator of the consistency of the changes in ENSO properties we found during the 20th century. The CMIP5 models also show different possible ENSO dynamics. Some of the models present some multidecadal variability but none of them fully agrees with the observed multidecadal changes in the ReOsc dynamics. However, the observed changes lie within all the possible dynamical states of ENSO represented by the models. Increasing uncertainties and errors in the observations back in time likely also contribute to the weaker recharge-oscillator mechanisms in the earlier periods. Such errors can increase noise amplitude in the model. This will increase the damping coefficients (a_{11} and a_{22}) and decrease the coupling coefficients (a_{12} and a_{21}), and it will weaken the cross-correlation between SST and WWV (see figure S6). Thus, the evolution of the ReOsc coefficients computed for our observational dataset is partly expected (see figure 3). Although all model coefficients show a certain degree of multidecadal variability, some of them seem to be partly affected by noise in the observations; mainly the damping coefficients a_{11} and a_{22}. The evolution of the coefficients representative of the coupling between SST and WWV (a_{12} and a_{21}) do not resemble the theoretical evolution of parameters affected by noise, as the strength of the coupling does not decrease monotonically back in time (figure 3), which indicates that the changes in the strength of the coupling could be real.

5. Conclusion

We show that the dynamics of ENSO can be explained by a mechanism of recharge-discharge of the equatorial heat content from the 1970s until 2010. The anomalies of the equatorial heat content strongly impact the SST anomalies with ten months lead. This has large implications for predictability of ENSO. ENSO is more predictable during the periods when the recharge-discharge mechanism dominates and we can use the equatorial heat content as a good predictor of ENSO.

Lastly, analysis of CMIP5 historical simulations indicates that rather than external factors, the multidecadal variability of ENSO dynamics presented in this study likely explains the changes in ENSO properties, but we acknowledge that observational uncertainties are large in the beginning of 20th century. Therefore our study has two plausible interpretations: (a) errors in our observational dataset prior to the 1960s lead to an apparent decadal variability and (b) the decadal variability present in our observational dataset is real but the CMIP models fail to capture it. Longer and more reliable observational records would be required to validate our results.

Data availability statement

The data that support the findings of this study are available upon reasonable request from the authors.

Acknowledgments

(archive.norstore.no). We temporarily provide a copy of the output data of the ReOsc model as supporting information.

ORCID iDs

Lander R Crespo ⬩ https://orcid.org/0000-0003-1273-4303

Mª Belén Rodríguez-Fonseca ⬩
https://orcid.org/0000-0002-5261-7083

Irene Polo ⬩ https://orcid.org/0000-0002-6250-6109

Noel Keenlyside ⬩ https://orcid.org/0000-0002-8708-6868

Dietmar Dommenget ⬩ https://orcid.org/0000-0002-5129-7719

References

An S-I 2009 A review of interdecadal changes in the nonlinearity of the El Niño-Southern Oscillation *Theor. Appl. Climatol.* **97** 29–40

An S-I and Jin F-F 2000 An eigen analysis of the interdecadal changes in the structure and frequency of ENSO mode *Geophys. Res. Lett.* **27** 2573–6

An S-I and Wang B 2000 Interdecadal change of the structure of the ENSO mode and its impact on the ENSO frequency *J. Clim.* **13** 2044–55

Annamalai H, Xie S P, McCreary J P and Murtugudde R 2005 Impact of Indian Ocean sea surface temperature on developing El Niño *J. Clim.* **18** 302–19

Behera S K, Luo J J, Masson S, Rao S A, Sakuma H and Yamagata T 2006 A CGCM study on the interaction between IOD and ENSO *J. Clim.* **19** 1688–705

Bellenger H, Guilyardi E, Leloup J, Lengaigne M and Vialard J 2014 ENSO representation in climate models: from CMIP3 to CMIP5 *Clim. Dyn.* **42** 1999–2018

Bjerknes J 1969 Atmospheric teleconnections from the equatorial Pacific *Mon. Weather Rev.* **97** 163–72

Bunge L and Clarke A J 2014 On the warm water volume and its changing relationship with ENSO *J. Phys. Oceanogr.* **44** 1372–85

Burgers G, Jin F-F and van Oldenborgh G J 2005 The simplest ENSO recharge oscillator *Geophys. Res. Lett.* **32** L13706

Cai W, Wu L, Lengaigne M, Li T, McGregor S and Kug J-S 2019 Pantropical climate interactions *Science* **363** eaav4236

Carton J A, Giese B S and Grodsky S A 2005 Sea level rise and the warming of the oceans in the Simple Ocean Data Assimilation (SODA) ocean reanalysis *J. Geophys. Res. Oceans* **110** C09006

Clement A, DiNezio P and Deser C 2011 Rethinking the ocean's role in the Southern Oscillation *J. Clim.* **24** 4056–72

de Boisséson E and Balmaseda M 2016 An ensemble of 20th century ocean reanalyses for providing ocean initial conditions for CERA-20C coupled streams ERA Report Series

Ding H, Keenlyside N S and Latif M 2012 Impact of the Eequatorial Atlantic on the El Nino southern oscillation *Clim. Dyn.* **38** 1965–72

Dommenget D, Semenov V and Latif M 2006 Impacts of the tropical Indian and Atlantic Oceans on ENSO *Geophys. Res. Lett.* **33** L11701

Dommenget D and Vijayeta A 2019 Simulated future changes in ENSO dynamics in the framework of the linear recharge oscillator model *Clim. Dyn.* **53** 4233–48

Dommenget D and Yu Y 2017 The effects of remote SST forcings on ENSO dynamics, variability and diversity *Clim. Dyn.* **49** 2605–24

Dong B, Sutton R T and Scaife A A 2006 Multidecadal modulation of El Niño–Southern Oscillation (ENSO) variance by Atlantic Ocean sea surface temperatures *Geophys. Res. Lett.* **33**

Fang X and Zheng F 2018 Simulating Eastern- and Central-Pacific type ENSO using a simple coupled model *Adv. Atmos. Sci.* **35** 671–81

Fedorov A V, Hu S, Wittenberg A T, Levine A F and Deser C 2020 ENSO low-frequency modulation and mean state interactions *El Niño Southern Oscillation in a Changing Climate* AGU Geophysical Monograph Series pp 173–98

Fedorov A V and Philander S G 2001 A stability analysis of tropical ocean–atmosphere interactions: bridging measurements and theory for El Niño *J. Clim.* **14** 3086–101

Feng J, Lian T, Ying J, Li J and Li G 2020 Do CMIP5 models show El Niño diversity? *J. Clim.* **33** 1619–41

Frauen C and Dommenget D 2012 Influences of the tropical Indian and Atlantic Oceans on the predictability of ENSO *Geophys. Res. Lett.* **39** L02706

Giese B S and Ray S 2011 El Niño variability in simple ocean data assimilation (SODA), 1871–2008 *J. Geophys. Res.* **116** C02024

Guilyardi E 2006 El Nino-mean state-seasonal cycle interactions in a multi-model ensemble *Clim. Dyn.* **26** 329–48

Ham Y-G, Kug J-S and Park J-Y 2013 Two distinct roles of Atlantic SSTs in ENSO variability: North Tropical Atlantic SST and Atlantic Niño *Geophys. Res. Lett.* **40** 4012–7

Hu Z-Z, Kumar A, Huang B, Zhu J, L'Heureux M, McPhaden M J and Yu J-Y 2020 The interdecadal shift of ENSO properties in 1999/2000: a review *J. Clim.* **33** 4441–62

Jansen M F, Dommenget D and Keenlyside N 2009 Tropical atmosphere–ocean interactions in a conceptual framework *J. Clim.* **22** 550–67

Jin F-F 1997a An equatorial ocean recharge paradigm for ENSO. Part I: conceptual model *J. Atmos. Sci.* **54** 811–29

Jin F-F 1997b An equatorial ocean recharge paradigm for ENSO. Part II: a stripped-down coupled model *J. Atmos. Sci.* **54** 830–47

Kajtar J B, Santoso A, McGregor S, England M H and Baillie Z 2018 Model under-representation of decadal Pacific trade wind trends and its link to tropical Atlantic bias *Clim. Dyn.* **50** 1471–84

Kirtman B P and Schopf P S 1998 Decadal variability in ENSO predictability and prediction *J. Clim.* **11** 2804–22

Kug J-S, Ham Y-G, Lee J-Y and Jin F-F 2012 Improved simulation of two types of El Niño in CMIP5 models *Environ. Res. Lett.* **7** 034002

Li X, Hu Z-Z, Huang B and Jin F-F 2020 On the interdecadal variation of the warm water volume in the tropical Pacific around 1999/2000 *J. Geophys. Res. Atmos.* **125** e2020JD033306

Li X, Xie S-P, Gille S T and Yoo C 2015 Atlantic-induced pan-tropical climate change over the past three decades *Nat. Clim. Change* **6** 275

Martín-Rey M, Rodríguez-Fonseca B and Polo I 2015 Atlantic opportunities for ENSO prediction *Geophys. Res. Lett.* **42** 6802–10

Martín-Rey M, Rodríguez-Fonseca B, Polo I and Kucharski F 2014 On the Atlantic–Pacific Niños connection: a multidecadal modulated mode *Clim. Dyn.* **43** 3163–78

McGregor S, Stuecker M F, Kajtar J B, England M H and Collins M 2018 Model tropical Atlantic biases underpin diminished Pacific decadal variability *Nat. Clim. Change* **8** 493–8

Philander S G and Fedorov A 2003 Is El Niño sporadic or cyclic? *Annu. Rev. Earth Planet. Sci.* **31** 579–94

Polo I, Martin-Rey M, Rodriguez-Fonseca B, Kucharski F and Mechoso C R 2015 Processes in the Pacific La Niña onset triggered by the Atlantic Niño *Clim. Dyn.* **44** 115–31

Polo I, Rodríguez-Fonseca B, Losada T and García-Serrano J 2008 Tropical Atlantic variability modes (1979–2002). Part I: time-evolving SST modes related to West African rainfall *J. Clim.* **21** 6457–75

Rayner N A, Parker D E, Horton E B, Folland C K, Alexander L V, Rowell D P, Kent E C and Kaplan A 2003 Global analyses of sea surface temperature, sea ice, and night marine air temperature since the late nineteenth century *J. Geophys. Res. Atmos.* **108**

Rodríguez-Fonseca B, Polo I, García-Serrano J, Losada T, Mohino E, Mechoso C R and Kucharski F 2009 Are Atlantic Niños enhancing Pacific ENSO events in recent decades? *Geophys. Res. Lett.* **36** L20705

Sciremammano F 1979 A suggestion for the presentation of correlations and their significance levels *J. Phys. Oceanogr.* **9** 1273–6

Suarez M J and Schopf P S 1988 A Delayed Action Oscillator for ENSO *J. Atmos. Sci.* **45** 3283–7

Taylor K E, Stouffer R J and Meehl G A 2012 An overview of CMIP5 and the experiment design *Bull. Am. Meteorol. Soc.* **93** 485–98

Timmermann A *et al* 2018 El Niño–Southern Oscillation complexity *Nature* **559** 535–45

Vijayeta A and Dommenget D 2018 An evaluation of ENSO dynamics in CMIP simulations in the framework of the recharge oscillator model *Clim. Dyn.* **51** 1753–71

Wang B and An S-I 2001 Why the properties of El Niño changed during the late 1970s *Geophys. Res. Lett.* **28** 3709–12

Wang B, Luo X, Yang Y-M, Sun W, Cane M A, Cai W, Yeh S-W and Liu J 2019 Historical change of El Niño properties sheds light on future changes of extreme El Niño *Proc. Natl Acad. Sci. USA* **116** 22512–7

Wang G, Cai W and Santoso A 2020 Stronger increase in the frequency of extreme convective El Niño than extreme warm El Niño under greenhouse warming *J. Clim.* **33** 675–90

Wang L, Yu J-Y and Paek H 2017 Enhanced biennial variability in the Pacific due to Atlantic capacitor effect *Nat. Commun.* **8** 14887

Wittenberg A T 2009 Are historical records sufficient to constrain ENSO simulations? *Geophys. Res. Lett.* **36**

Wu R and Kirtman B P 2004 Understanding the impacts of the Indian Ocean on ENSO variability in a coupled GCM *J. Clim.* **17** 4019–31

Yeh S-W and Kirtman B P 2004 Tropical Pacific decadal variability and ENSO amplitude modulation in a CGCM *J. Geophys. Res.* **109**

Yeh S-W, Wu R and Kirtman B P 2007 Impact of the Indian Ocean on ENSO variability in a hybrid coupled model *Q. J. R. Meteorol. Soc.* **133** 445–57

Yu J-Y, Mechoso C R, McWilliams J C and Arakawa A 2002 Impacts of the Indian Ocean on the ENSO cycle *Geophys. Res. Lett.* **29** 46-1–46-4

Zanchettin D, Bothe O, Graf H F, Omrani N E, Rubino A and Jungclaus J H 2016 A decadally delayed response of the tropical Pacific to Atlantic multidecadal variability *Geophys. Res. Lett.* **43** 784–92